Journal Name

ARTICLE TYPE

Bifunctional electrocatalytic activity of Fe-embedded biphenylene for oxygen reduction and evolution reactions

Junkai Xu,[a‡] Yang Gao,[a‡] Jing Li,[a] Xun-Wang Yan,[*a] and Fengjie Ma [*b]

1 Electronic supplementary information

1.1 Computational Methods

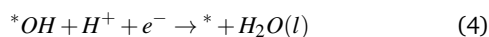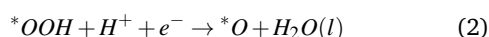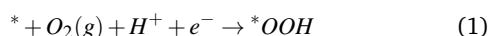#### 1.1.1 DFT calculations

The calculations are performed in VASP package, in which the plane wave pseudopotential method and the projector augmented-wave (PAW) pseudopotential with Perdew-Burke-Ernzerhof (PBE) functional are adopted[1–4], and also the GGA + U method is employed to consider the correction of electron correlation[5]. The U values for FeN_4-, CoN_4-, and NiN_4-biphenylene are 4.47 eV, 6.00 eV, and 5.80 eV, respectively, which are determined by the linear response method enclosed in the examples in VASP package. The plane wave basis cutoff is 500 eV and the thresholds are 10^{-5} eV and 0.02 eV/Å for total energy and force convergence. The inter-layer distance was set to 20 Å and a mesh of $9 \times 7 \times 1$ k-points is used for the Brillouin zone integration. In the ab initio molecular dynamics simulations, the temperature was kept at 500 K for 10 ps with a time step of 1 fs in the canonical ensemble (NVT)[6].

1.1.2 Free energy changes

Under the acid condition (PH = 0), we study the ORR on MN_4-biphenylene, which is assumed to be a four-electron pathway[7]. In the first step, MN_4-biphenylene captures one O_2 molecule and a pair of proton and electron ($H^+ + e^-$) to form $^*OOH$. Then, $^*OOH$ combines another pair of H^+ and e^- to generate $^*O$ and release one H_2O molecule. Next, $^*O$ continuously combines one ($H^+ + e^-$), leading to the formation of $^*OH$. Finally, as one pair of H^+ and e^- comes again, another H_2O molecule is generated, corresponding to the termination of the reaction loop. The four elementary steps of ORR can be described as:

$$^* + O_2(g) + H^+ + e^- \rightarrow {}^*OOH \tag{1}$$

$$^*OOH + H^+ + e^- \rightarrow {}^*O + H_2O(l) \tag{2}$$

$$^*O + H^+ + e^- \rightarrow {}^*OH \tag{3}$$

$$^*OH + H^+ + e^- \rightarrow {}^* + H_2O(l) \tag{4}$$

where the g and l denote the gas phase and liquid phase respectively, and the * denotes MN_4-biphenylene. Herein, the free energy of O_2 is from the experimental reaction energy of O_2 + $2H_2$ → $2H_2O$ (-4.92 eV). In addition, under standard hydrogen electrode conditions, the energy of the ($H^+ + e^-$) pair can be replaced by half of the free energy of the H_2 molecule at 298.15 K[8]. Then, the free energy change of each step can be written as:

$$\Delta G_1 = G_{*OOH} - G_* - G_{O_2} - \frac{1}{2}G_{H_2} \tag{5}$$

$$\Delta G_2 = G_{*O} + G_{H_2O} - G_{*OOH} - \frac{1}{2}G_{H_2} \tag{6}$$

$$\Delta G_3 = G_{*OH} - G_{*O} - \frac{1}{2}G_{H_2} \tag{7}$$

$$\Delta G_4 = G_* + G_{H_2O} - G_{*OH} - \frac{1}{2}G_{H_2} \tag{8}$$

where the G_*, G_{*O}, G_{*OH} and G_{*OOH} are the free energies of *, $^*O$, $^*OH$ and $^*OOH$, respectively. G_{H_2O}, G_{O_2}, and G_{H_2} are the free energies of H_2O, O_2, and H_2 molecules, respectively. The Gibbs free energy was calculated in terms of the equation[9],

$$G = E + ZPE + \Delta U - TS, \tag{9}$$

in which E is the total energy from DFT calculation, ZPE is zero-point energy, ΔU is the change of internal energy from 0 K to 298.15 K, and TS is the entropy at 298.15 K. The step with the greatest change of energy is defined as the potential-determining

^{a} College of Physics and Engineering, Qufu Normal University, Qufu, Shandong 273165, China
^{b} The Center for Advanced Quantum Studies and Department of Physics, Beijing Normal University, Beijing 100875, China.
∗ Corresponding authors: yanxunwang@163.com; fengjie.ma@bnu.edu.cn.

reaction step (PDS). To evaluate the catalytic activity, the ORR and OER overpotentials are defined as:

$$\eta_{ORR} = \frac{\max{(\Delta G_1, \Delta G_2, \Delta G_3, \Delta G_4)}}{e} + 1.23 \qquad (10)$$

$$\eta_{OER} = \frac{\max{(-\Delta G_1, -\Delta G_2, -\Delta G_3, -\Delta G_4)}}{e} - 1.23 \quad (11)$$

1.1.3 Hubbard U value

A linear-response approach to determine the U parameter had been proposed by M. Cococcioni and S. de Gironcoli[10], and the method is contained in the example category "Calculate U for LSDA +U" on the Vaspwiki website. The linear response function is the number of d electrons on the transition metal atom with respect to the perturbation potential. The self-consistent and non-self-consistent calculations of single-point energy are performed at a few values of non-zero perturbation potentials. Then, the numbers of d electrons are collected and displayed in Fig. S1. Finally, the U values are computed by the formula $U = 1/k_{scf} - 1/k_{nscf}$, where k_{scf} and k_{nscf} are the slopes of linear functions. The Hubbard U values are 4.47 eV, 6.00 eV, and 5.80 eV for the Fe-, Co-, and Ni-embedded biphenylene in our calculations.
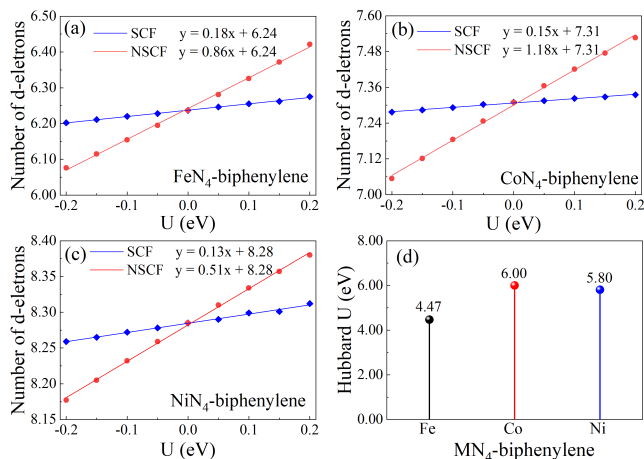

Fig. S1 (a)-(c) The variation of the number of d electrons on the transition metal atom with respect to the perturbation potential for Fe-, Co-, and Ni-embedded biphenylene. (d) Hubbard U values.

1.2 Molecular dynamics simulation

The molecular dynamics calculations are performed with the temperature parameter 500 K and the time parameter 10 ps. The total potential energies fluctuate around a certain value and no distinct drop occurs, shown in Fig. S2. The inserts are the top and side views of the final configurations for the three MN$_4$-biphenylenes, which indicate that the structures have changed very little and no chemical bonds are broken. Hence, the MN$_4$-biphenylene SACs (M = Fe, Co, and Ni) are thermally stable.

1.3 Dissociation mechanism of O$_2$ reduction

In the ORR reactions on the Fe-doped biphenylene, the associative mechanism is dominant. To clarify this, we compute and
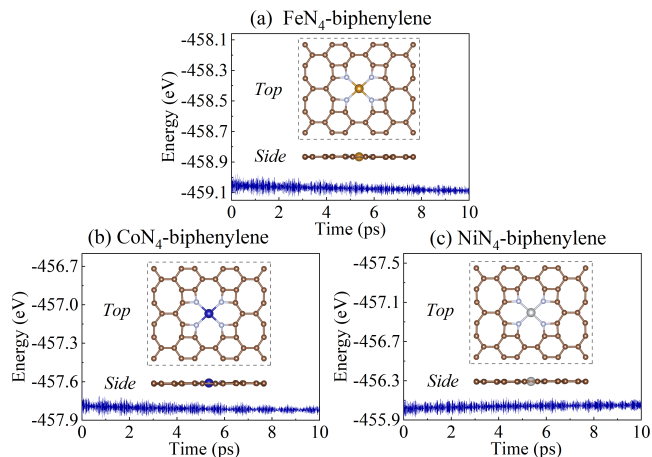

Fig. S2 In the molecular dynamics simulations at 500 K, the total potential energies of the three MN$_4$-biphenylene systems fluctuate around a certain value. The inserts are top and side views of the final configurations after 10 ps.

compare the energies of O$_2$-adsorbed systems with different adsorption sites on the catalyst surface. Fig.S3 displays the possible adsorption sites on the Fe-embedded biphenylene. There are two
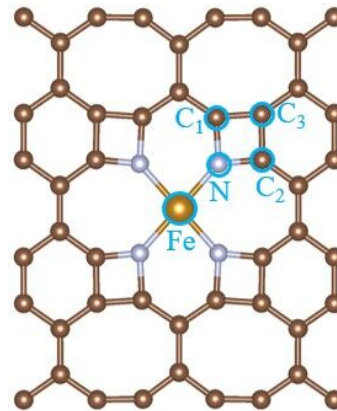

Fig. S3 Possible adsorption sites of O$_2$ molecule.

types of O$_2$ adsorption. One is vertical adsorption that only one O atom of the O$_2$ molecule is linked to the slab. In our calculations, the energies are -469.82 eV and -468.87 eV with O$_2$ vertically adsorbed on the Fe site and the C$_1$ site, respectively. The N, C$_2$, and C$_3$ sites are not favorable adsorption sites because the O$_2$ molecule will move away from these sites in the process of relaxation calculations. Another type of O$_2$ adsorption is parallel adsorption that two O atoms are linked to two atoms of the slab. For the N-C$_1$ and N-C$_2$ sites, the O$_2$ molecule does not bond on them after the structure relaxation in the calculations. The corresponding energies are listed in Table. 1 below. By comparing these energies, we can find that the system with O$_2$-adsorbed on the Fe site with vertical adsorption configuration has lower energy than other adsorption configurations, indicating that the Fe site rather than the C site of the four-membered ring is the active site. Hence, we can determine that the associate mechanism is

dominated in the ORR process in terms of the O_2 vertical adsorption.

Table 1 The Energies of O_2-adsorbed systems in the parallel pattern.

Site	Fe-N	N-C_1	N-C_2	C_1-C_2	C_1-C_3	C_2-C_3
Energy (eV)	-469.07	/	/	-468.65	-469.53	-469.44

To confirm the above conclusion, we also do a transition state calculation. The initial state is shown in Fig. S4(a) with the O_2 molecule adsorbed on the Fe site. The final state is shown in Fig. S4(c) where two O atoms have been dissociated and attached to the Fe site and the C site separately. The energy barrier is 1.52 eV shown in Fig. S5, which is large enough to hamper the dissociation of O_2 molecule. It is noted that the one of O atoms is just located at N site in the transition state in Fig. S4(b). N site is not the favorite site for O adsorption. The fact prevents the decomposition of O_2 molecule related to the dissociation mechanism.
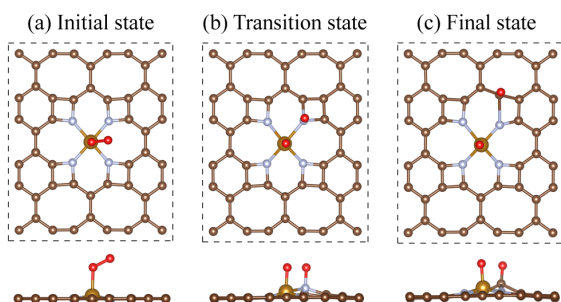

Fig. S4 Dissociation process of O_2 molecule. (a) Initial state, (b) Transition state, (c) Final state.
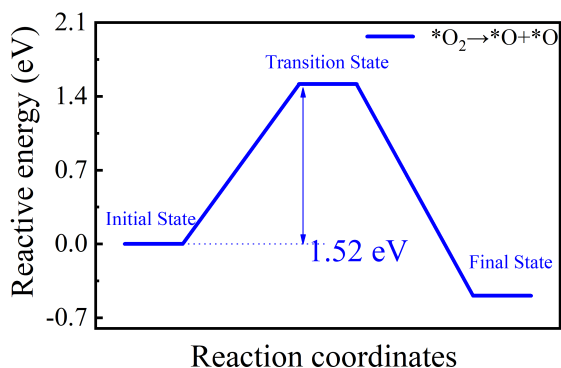

Fig. S5 The energy barrier of the dissociation of O_2 molecule on catalytic surface.

Fig. S6 Structural configurations of initial state, transition state, and final state. (a) $^*O_2 + H \rightarrow {}^*OOH$, (b) $^*OOH + H \rightarrow {}^*O + H_2O$, (c) $^*O + H \rightarrow {}^*OH$, (d) $^*OH + H \rightarrow {}^* + H_2O$.

1.4 The process of the proton transfer in the four ORR steps

In each step of O_2 reduction, the initial state (IS), transition state (TS), and final state (FS) of proton transfer on the catalytic surface are shown in Fig. S6. In the initial state, H is on the top of N atom. Then, H moves to the intermediates to react in the four elementary steps.
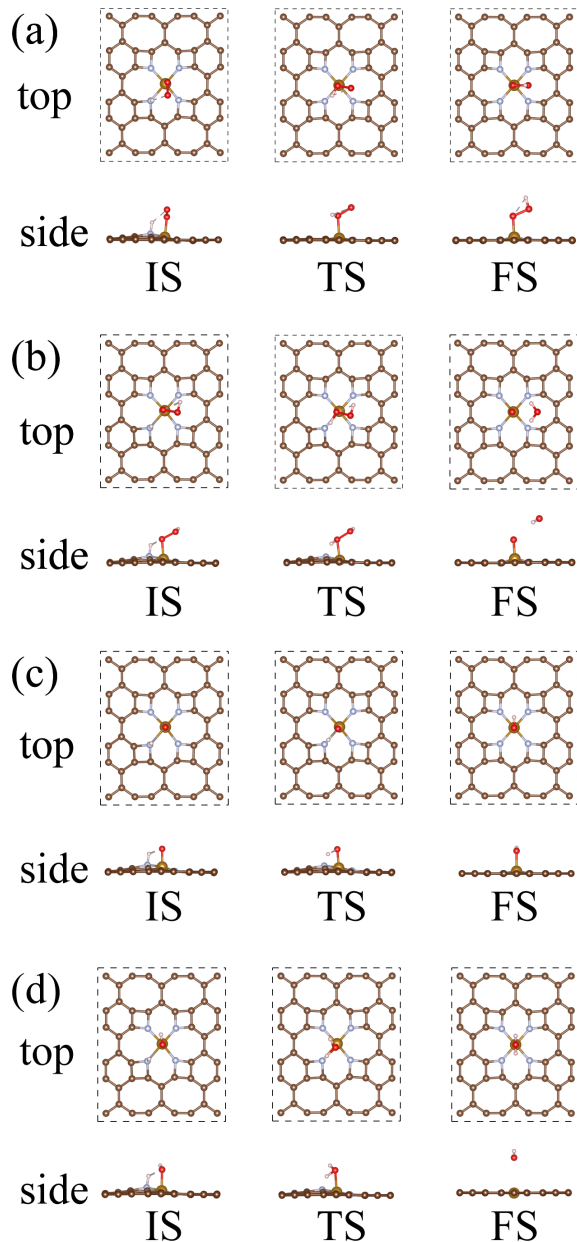
1.5 The negative COHP diagrams

The crystal orbital Hamilton population (COHP) is adopted to analyze the strength of the M-O bonds in the *OH and *OOH structures. The two intermediate phases are closely related to the PDS in the ORR or OER process, and further play a decisive role in the determination of overpotentials.
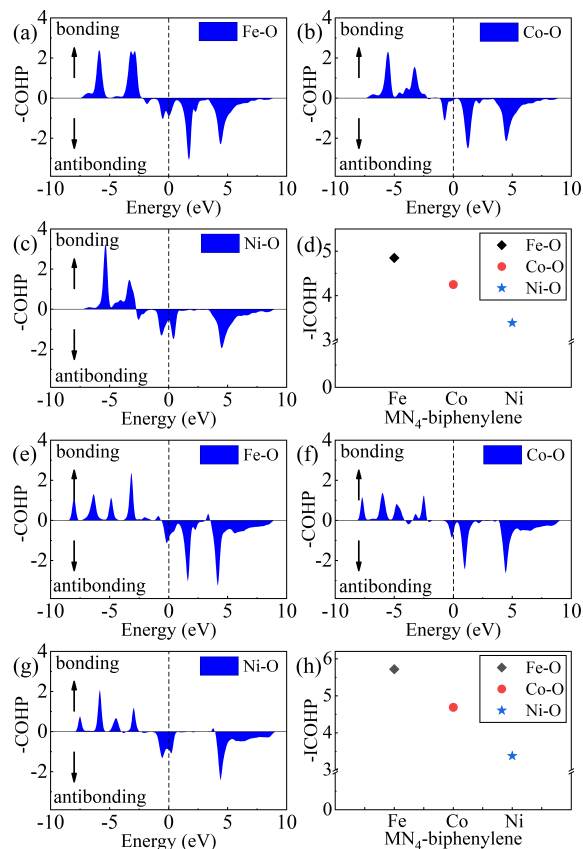

Fig. S7 -COHP of the bond M-O (M = Fe, Co, and Ni) in the composites of *OH and their -ICOHP value are displayed in (a)-(d). -COHP of the bond M-O (M = Fe, Co, and Ni) in the composites of *OOH and their -ICOHP value are displayed in (e)-(h). The Fermi energy is set to zero.

Notes and references

1 G. Kresse and J. Hafner, *Physical Review B*, 1993, **47**, 558–561.
2 G. Kresse and J. Furthmüller, *Physical Review B*, 1996, **54**, 11169–11186.
3 J. P. Perdew, K. Burke and M. Ernzerhof, *Physical Review Letters*, 1996, **77**, 3865–3868.
4 P. E. Blöchl, *Physical Review B*, 1994, **50**, 17953–17979.
5 M. Cococcioni and S. de Gironcoli, *Physical Review B*, 2005, **71**, 035105.
6 G. J. Martyna, M. L. Klein and M. Tuckerman, *The Journal of Chemical Physics*, 1992, **97**, 2635–2643.
7 G. Gao, E. R. Waclawik and A. Du, *Journal of Catalysis*, 2017, **352**, 579–585.
8 J. K. Nørskov, J. Rossmeisl, A. Logadottir, L. Lindqvist, J. R. Kitchin, T. Bligaard and H. Jónsson, *The Journal of Physical Chemistry B*, 2004, **108**, 17886–17892.
9 V. Wang, N. Xu, J.-C. Liu, G. Tang and W.-T. Geng, *Computer Physics Communications*, 2021, **267**, 108033.
10 M. Cococcioni and S. de Gironcoli, *Physical Review B*, 2005, **71**, 035105.